CONTROL ALLOCATION STRATEGIES
FOR AN OVERACTUATED ELECTRIC VEHICLE

J.-Y. Dieulot

LAGIS, Polytech-Lille/IAAL, Cité Scientifique, 59650 Villeneuve d'Ascq, France phone: 33-3-28-76-74-95
jean-yves.dieulot@polytech-lille.fr

ABSTRACT

Overactuated Intelligent Autonomous Electric Vehicles may possess up to 6 degrees of freedom, such as two steering devices and four independent traction wheels, which serve to control yaw, lateral and longitudinal velocities. It is shown that the coupled nonlinear control problem can be set as an optimal control strategy, which consists of a distribution of contact forces or steering angles according to yaw and lateral speed control. Then, the motor torques of the DC drives are computed in order to ensure dominant wheel rolling operation for a 4 X 4 motion or to ensure that all wheels are in the rolling state when using steering angles

Keywords: Hybrid Vehicle, Nonlinear Control, Control Allocation, Contract forces, Vehicle Steering

1. INTRODUCTION

Intelligent autonomous vehicles (IAVs) is a class of intelligent transportation systems which are operated without a human driver. As an example, these vehicles can be used in harbor environments for goods low-speed transportation, where they ensure safe, reconfigurable and, while electric, low emission traffic (Djeziri et al., 2009). Often, such vehicles embed multi-actuated traction and steering systems, which allows to consider redundancy in control, design of different scenarios to run the vehicle on a segment of the road, and control/operating modes reconfigurable solutions. A good knowledge of the kinematics and dynamics is important to design a robust MIMO controller of such intelligent autonomous vehicles, in order to compensate for external perturbations and local nonlinearities (Merzouki et al., 2007, Merzouki et al., 2009).

Since the 1980s, various active chassis vehicle control approaches have been investigated, some of which can be transposed to IAVs. In particular, research into vehicle dynamics control (VDC) or vehicle stability control systems has become very active (e.g. Furukawa and Abe, 1997). Variables to be controlled are typically longitudinal velocity, lateral velocity, and yaw rate, while the actuation generally includes individual wheel drive and steering devices. Recently, control allocation approaches have been introduced into vehicle control systems to take advantage of actuator redundancy for improving system performance and achieving reconfigurable control solutions e.g. Wang and Logoria (2009), Tjonnas and Johansen (2010). A control allocation approach is generally used when different combinations of effector commands can produce the same result and when the number of effectors available exceeds the number of states being controlled. In these suggested control allocation (CA) schemes, the generalized forces are allocated to longitudinal and/or lateral tire forces. Different CA schemes have been proposed, either by optimal control, nonlinear control or fuzzy logic e.g. Raffo et al (2009), Feiqiang et al. (2009), Partouche et al., (2007), Tjønnås and Johansen (2010) and very few on IAVs.

Vehicle motion is governed by forces induced by each tire interacting with the road, and these forces mainly depend on the slip velocity/slip angle and tire-friction coefficient Canudas de Wit et al.(2003), Merzouki et al. (2007), Bakker et al. (1989). While allocating the control effort to tires, it is important to take these factors into account, to ensure that the tire can actually yield the desired forces.

This study focuses mainly on the control of an over-actuated autonomous electric vehicle, using simplified dynamic and kinematic models (Djeziri et al., 2009). The developed dynamics concerns the longitudinal, lateral, vertical and yaw of the chassis, including the dynamics of the electromechanical systems and the wheel-ground interactions. Two kinds of control strategies are proposed, whether the automated steering systems are used or not.
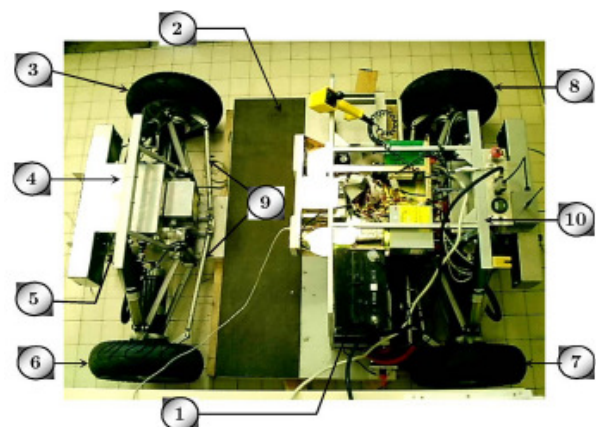
2. VEHICLE MODELLING

Figure 1: Robucar vehicle and actuators

The autonomous overactuated electric vehicle in Fig. 1, named Robucar, owns four actuated traction wheels and two actuated steering systems with a total of 6 degrees of freedom, thus allowing to handle actuator or sensor

defaults. Figure 1 shows the following composition : 1) 12-V 60-Ah sealed batteries; 2) a honeycomb chassis; 3) a front right wheel; 4) a front control cabinet; 5) a front steering electrical jack; 6) a front left wheel; 7) a rear left wheel; 8) a rear right wheel; 9) a rear steering electrical jack; and 10) a rear control cabinet. All technical details are supplied in previous papers (see e.g. Djeziri et al., 2009).

Basically, the overall model can be split up into 4 parts: the kinematic model, the behaviour of the chassis along the trajectory, the electromechanical model which links the motor voltage to the wheel speed and contact forces, and the modelling of the wheel-tire-road contact itself.
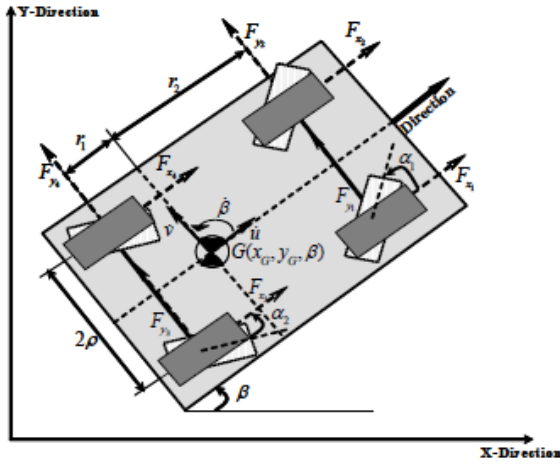
2.1. Chassis dynamics

Figure 2 Contact forces and kinematic parameters

Owing to the low vehicle velocity (< 20 km/h), all centrifugal forces are neglected in the sequel and only the longitudinal, lateral and yaw dynamics are considered which yields:

Longitudinal dynamics :
$$m\ddot{u} = (F_{x1} + F_{x2})\cos\alpha_1 + (F_{x3} + F_{x4})\cos(\alpha_2)$$
$$- (F_{y1} + F_{y2})\sin(\alpha_1) + (F_{y3} + F_{y4})\sin(\alpha_2) \qquad (1)$$

Lateral dynamics :
$$m\ddot{v} = (F_{x1} + F_{x2})\sin\alpha_1 - (F_{x3} + F_{x4})\sin(\alpha_2)$$
$$+ (F_{y1} + F_{y2})\cos(\alpha_1) + (F_{y3} + F_{y4})\cos(\alpha_2) \qquad (2)$$

Yaw dynamics :
$$I\ddot{\beta} = \left[(F_{x1} + F_{x2})\sin\alpha_1 + (F_{y1} + F_{y2})\cos(\alpha_1) \right] x_2$$
$$+ \left[(F_{x3} + F_{x4})\sin(\alpha_2) - (F_{y3} + F_{y4})\cos(\alpha_2) \right] x_1 \qquad (3)$$
$$+ \frac{\rho}{2} \left[\begin{array}{c} (F_{x1} - F_{x2})\cos\alpha_1 + (F_{x3} - F_{x4})\cos(\alpha_2) \\ - (F_{y1} - F_{y2})\sin(\alpha_1) + (F_{y3} - F_{y4})\sin(\alpha_2) \end{array} \right]$$

where $u, v, \beta, \alpha_1, \alpha_2$ are respectively the center of mass longitudinal, lateral speeds, yaw angle, back and rear

steering angles, F_{xi}, F_{yi} the longitudinal and lateral contact (tire) forces, I is the moment of inertia of the C.O.G with respect to the vertical axis, ρ is the axle track and m is the vehicle mass (Figure 2).

2.2. Kinematics

The heading, velocities and position of the vehicle in the absolute frame can be obtained using :

$$\dot{x}_G = \dot{u}\cos\beta - \dot{v}\sin\beta$$
$$\dot{y}_G = \dot{u}\sin\beta + \dot{v}\cos\beta$$

and the positions and yaw angle can be obtained by integration.

2.3. Electromechanical Model

The electromechanical model of a quarter-Robucar can be represented as a DC drive monitoring a two-mass-spring damper system which figures out the mechanical flexibilities of the transmission system, i.e., neglecting the current loop (with fast dynamics):

$$J_{ej}\ddot{\theta}_{ej} = -f_{ej}\dot{\theta}_{ej} - K_j (\theta_{ej} - N_j\theta_{sj}) + \Gamma_j$$
$$J_{sj}\ddot{\theta}_{sj} = -f_{sj}\dot{\theta}_{sj} + K_j N_j (\theta_{ej} - N_j\theta_{sj}) - \upsilon F_{xj} \qquad (4)$$

where θ_{ej}, θ_{sj} are the motor and wheel angle, Γ_j is the electrical motor torque, $J_{ej}, J_{sj}, f_{ej}, f_{sj}, K_j$ are the corresponding modal inertias, frictions and elasticity constants of the motor-wheel system, υ is the wheel radius, N_j is the speed ratio.

2.4. Modelling road-tire contact

As pointed out before, there are many ways to describe the tire-road modelling. Basically, one can introduce the slip velocity $\dot{x}_{sj} = \dot{u} - \upsilon\dot{\theta}_{sj}$, where υ is the wheel radius. The longitudinal effort can be estimated using such different models as the LuGre model (Canudas de Wit et al., 2003), the well-known Pacejka model (Bakkeer et al., 1989) or other models embedding a combination of different phenomena (Merzouki et al., 2007). Let the longitudinal forces be described by the Pacejka model for which:

$$G = (\upsilon\dot{\theta}_{sj} - \dot{x}_{sj}) / \max(\upsilon\dot{\theta}_{sj}, \dot{x}_{sj}) \qquad ,$$
$$F_{xj} = f(G)$$
$$= D\sin\{C\arctan[Bx - E(Bx - Arc\tan(Bx))]\} + S_v \qquad (5)$$

where F_{xj} is a so-called « canonical » curve, and the parameters A, B, C, D, E, S_v depend on external conditions. (Fig. 3)

2.5. Available Measurements & state reconstruction

To improve the efficiency of intelligent and autonomous vehicle, the following information should be determined and available in real time (Djeziri et al., 2009):

1. Position localization of the vehicle;
2. Kinematic and dynamic states of the vehicle;
3. Evolutive state of the environment surrounding the vehicle;
4. State of the traction and steering controls in presence of obstacles or referred targets;
5. Communication between vehicle to vehicle or vehicle to infrastructure;
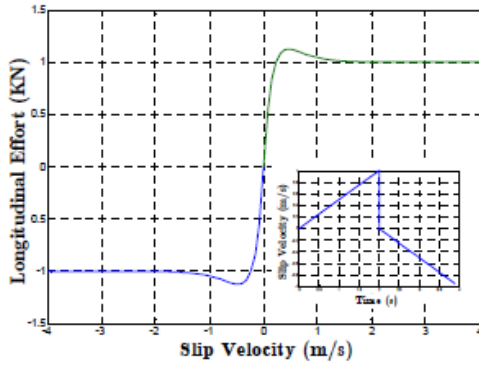6. Access to the coordinates of the trajectory.

Figure 3. Canonical contact forces curve

On the *Robucar* system, a GPS system ensures the localization of the vehicle whereas optical encoders and accelerometers allow to yield wheel and motors position, speed and accelerations. Some variables as the contact forces and the real transmitted torque have to be estimated using a state observer based on second-order sliding mode (Merzouki et al., 2009). Nevertheless, every variable in the previous and remaining equations can be either measured, or estimated (Djeziri et al., 2009).

3. CONTROL STRATEGIES

Generally speaking, monitoring a fully automated vehicle which purposes are goods transportation should meet the following requirements :

- track a geometric trajectory $g(x_c, y_c) = 0$ with a required tolerance
- use the vehicle safely (e.g. beware of tire-road contact, obstacle such as steps); this includes yaw and lateral velocity control
- embed all electromechanical constraints
- given all constraints, operate at maximum longitudinal velocity.

Details about the trajectory and contact forces are given in Fig. 4. Monitoring an autonomous electric vehicle can thus be viewed as an optimal control under constraints. This paper presents preliminary results where driving along a straight road $y_c = 0$ is only considered. The optimal control along the road can thus be formulated as follows:

$$\max x(t)$$

$$s.t. \ \lim_{t \to \infty} \beta = 0, \lim_{t \to \infty} y = 0$$

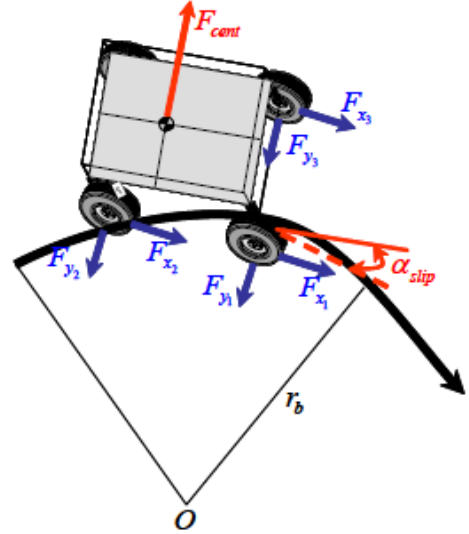$$\left| \dot{x}(t) \right| \le V_{max}, \left| u(t) \right| \le U_{max}$$

Figure 4. Motion and contact forces

3.1. 4 X 4 actuation with dominant wheel

The basic idea of the control scheme is to use the traction wheels control, by letting a combination of contact forces ensure an appropriate control of the yaw and lateral speed (see Figures 6-7) . The remaining degrees of freedom are available to ensure that at least one wheel operates in the rolling stage.

3.1.1. Hierarchical control

From (1-2), one has

$$m\ddot{u} \cos\left(\frac{\alpha_2 - \alpha_1}{2}\right) + m\ddot{v} \sin\left(\frac{\alpha_2 - \alpha_1}{2}\right) =$$

$$\left(F_{x1} + F_{x2}\right) \cos\alpha_1 \cos\left(\frac{\alpha_2 - \alpha_1}{2}\right) +$$

$$\left(F_{x3} + F_{x4}\right) \cos\left(\frac{\alpha_2 - \alpha_1}{2}\right) \cos(\alpha_2) +$$

$$+\left(F_{x1} + F_{x2}\right) \sin\alpha_1 \sin\left(\frac{\alpha_2 - \alpha_1}{2}\right)$$

$$-\left(F_{x3} + F_{x4}\right) \sin\left(\frac{\alpha_2 - \alpha_1}{2}\right) \sin(\alpha_2)$$

and

$$mü\cos\left(\frac{\alpha_2-\alpha_1}{2}\right)+m\ddot{v}\sin\left(\frac{\alpha_1-\alpha_2}{2}\right)=$$

$$\left(F_{x1}+F_{x2}\right)\cos\left(\frac{\alpha_2+\alpha_1}{2}\right)+\left(F_{x3}+F_{x4}\right)\cos\left(\frac{\alpha_2+\alpha_1}{2}\right)\qquad(6)$$

One can draw the following chassis control strategy:

- yaw control using $\Delta F_x = F_{x1} - F_{x2} = F_{x3} - F_{x4}$ as input
- lateral speed control using
  $\sum F_x = F_{x1} + F_{x2} + F_{x3} + F_{x4}$ as input
- maximum speed control $Vx = \dot{u}$
  using $F_x^+ = \sup\{F_{xi}\}$ as input

When $F_x^+ = \sup\{F_{xi}\}$ is known, the other forces can be allocated and, then, every motor torque can be derived.

- Lateral speed control

Using lateral and longitudinal acceleration feedbacks, one yields $\sum F_x$

$$\left(\sum F_x\right)\cos\left(\frac{\alpha_2+\alpha_1}{2}\right)=m\ddot{u}\cos\left(\frac{\alpha_2-\alpha_1}{2}\right)$$
$$+k_v^v m\dot{v}\sin\left(\frac{\alpha_1-\alpha_2}{2}\right)+k_v^x mv\sin\left(\frac{\alpha_1-\alpha_2}{2}\right)\qquad(7)$$

which ensures the closed-loop lateral speed dynamics:

$\ddot{v}+k_v^v\dot{v}+k_v^x v=0$ and $\lim\limits_{t\to\infty}v\to0$, where k_v^v,k_v^x are adequately chosen.

- Yaw control

In equation (3), the first group of terms is related to the lateral behavior, which is enforced to zero by equation (7). Hence, *only the slip phenomenon is accounted for,* which simplifies equation (3) to:

$$I\ddot{\beta}=\frac{\rho}{2}\Delta F_x\left[\cos\alpha_1\cos\left(\alpha_2\right)\right]\qquad(8)$$

and ΔF_x can be deduced easily

$$\frac{\rho}{2}\Delta F_x\left[\cos\alpha_1\cos\left(\alpha_2\right)\right]=I\dot{\beta}k_\beta^v+I\beta k_\beta^x,\qquad(9)$$

Hence, the controlled yaw dynamics is

$I\ddot{\beta}+I\dot{\beta}k_\beta^v+I\beta k_\beta^x=0$,

which, when coefficients k_β^x,k_β^v are adequately chosen, ensures the yaw closed-loop dynamics to converge to zero, $\lim\limits_{t\to\infty}\beta\to0$

3.1.2. Estimation of contact forces

Let us suppose, for example, that the dominant side is the left one, that the same difference $\Delta F_x = F_{x1} - F_{x2} = F_{x3} - F_{x4}$ applies. If one can find the

adequate dominant contact force, say F_{x1}, the other desired forces can be deduced in real time from (8-9), as summed up in Figure 6. The next goal is then to be able to monitor the dominant force and the other forces, which depend on the tire-road contact, for a quarter-car. This aspect is handled in paragraph 3.3.

3.2. Non-slip condition using steering actuators

As the vehicle is overactuated, it could be possible to use the steering actuators to monitor both yaw and lateral speed. In this case, the used method consists of lettings all wheels converge to the rolling (non-slip) stage (Figure 5).
In this case, one can simplify equations (2-3) to:

$$m\ddot{v}\approx\left(F_{x1}+F_{x2}\right)\sin\alpha_1-\left(F_{x3}+F_{x4}\right)\sin\left(\alpha_2\right)$$

$$I\ddot{\beta}=\frac{\rho}{2}\left[\left(F_{x1}-F_{x2}\right)\cos\alpha_1+\left(F_{x3}-F_{x4}\right)\cos\left(\alpha_2\right)\right]$$

Adequate control can be obtained using lateral and yaw acceleration feedback:

$$\left(\hat{F}_{x1}+\hat{F}_{x2}\right)\sin\alpha_1-\left(\hat{F}_{x3}+\hat{F}_{x4}\right)\sin\left(\alpha_2\right)=$$
$$m\left(k_v^v\dot{v}+k_v^x v\right)$$

$$\frac{\rho}{2}\left[\left(F_{x1}-F_{x2}\right)\cos\alpha_1+\left(F_{x3}-F_{x4}\right)\cos\left(\alpha_2\right)\right]=$$
$$I\left(k_\beta^v\dot{\beta}+k_\beta^x\beta\right)\qquad(10)$$

which yields :

$$\ddot{v}+k_v^v\dot{v}+k_v^x v=0$$
$$\ddot{\beta}+\dot{\beta}k_\beta^v+\beta k_\beta^x=0$$

where parameters $k_{(.)}^{(.)}$ are adequately chosen to ensure the convergence of v,β to zero

Of course, one has to solve equation (10), which will consists of finding the roots of a 4th order polynomial at each time (one can transform this set of equations into two polynomials using the transformation in $\tan\left(\frac{\alpha_i}{2}\right)$).

On a straight line, if $\left(F_{x1}-F_{x2}\right)=\left(F_{x3}-F_{x4}\right)=0$, equation (10) may have no solution, and, in this case, it is necessary that at least one of the wheels be in slip stage.

3.3. Control of a wheel with rolling condition

3.3.1. Dominant wheel control

In order to accelerate properly, one would like to obtain a slip value $G\to0$ so that $\dot{x}-v\dot{\theta}_{sj}\to0$

Let us not forget that, in practice, $|\dot{x}| = |\dot{u}| \leq V_{\max}$ where $V_{\max}$ is the maximum speed of the vehicle.

Combining the two equations in (4) yields, neglecting viscous friction::

$$N_j J_{ej} \ddot{\theta}_{ej} + J_{sj} \ddot{\theta}_{sj} = N_j \Gamma_j - \upsilon F_{xj} \tag{11}$$
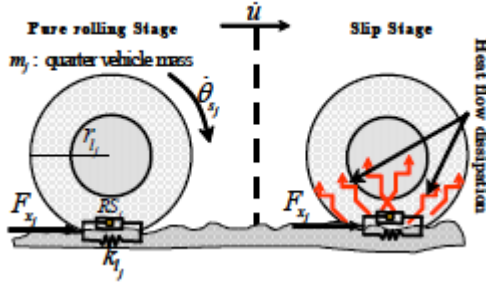

Figure 5. Rolling and slip stages

Acceleration feedback is a powerful control structure which allows to eliminate the vibration mode of such linear flexible systems at the expense of mounting acceleration sensors on the wheels and motor (see (Dieulot and Colas, 2009; Dumetz et al., 2006) for practical demonstrations on 2-mass-spring systems):

$$N_j \Gamma_j = N_j J_{ej} \ddot{\theta}_{ej} + J_{sj}\left(-\ddot{x}/\upsilon\right)$$
$$+ k_{\upsilon}^y J_{sj}\left(\dot{\theta}_{sj} - \dot{x}/\upsilon\right) + k_{\upsilon}^x J_{sj}\left(\theta_{sj} - x/\upsilon\right) + \upsilon \hat{F}_{xj} \tag{12}$$

where $\hat{F}_{xj}$ is the estimate of F_{xj}.

Controller (12) ensures that:

$$\left(\ddot{\theta}_{sj} - \ddot{x}/\upsilon\right) + k_{\upsilon}^y\left(\dot{\theta}_{sj} - \dot{x}/\upsilon\right) + k_{\upsilon}^x\left(\theta_{sj} - x/\upsilon\right) = 0 \tag{13}$$

and thus that $G \to 0$.

This methodology can be applied for the dominant wheel when not using steering commands or for each wheel, independently, when using steering commands.

3.3.2. Slave wheels control

In the case where steering actuators are not used, slave forces are given by (8-9), and the goal is to ensure convergence of the corresponding slip angle $x - \upsilon\theta_{sj}$ of the jth wheel to the appropriate one, using the model given in (5).

In the same way as before, since

$$N_j J_{ej} \ddot{\theta}_{ej} + J_{sj} \ddot{\theta}_{sj} = N_j \Gamma_j - \upsilon F_{xj} . \tag{14}$$

One wants that $F_{xj} = \tilde{F}_{xj}$.

Equation (5) or the canonical curve deriving from it provides us with a slip reference $\left(\dot{x} - \upsilon\dot{\theta}_s\right)_{ref}$ which corresponds to the computed reference contact force $\hat{F}_{xj}$ and then one should have:

$$N_j \Gamma_j = N_j J_{ej} \ddot{\theta}_{ej} + J_{sj} \ddot{\theta}_{sj} + J_{sj}\overline{\left(\ddot{\theta}_{sj} - \ddot{x}/\upsilon\right)}$$
$$+ k_{\upsilon}^y J_{sj}\overline{\left(\dot{\theta}_{sj} - \dot{x}/\upsilon\right)} + k_{\upsilon}^x J_{sj}\overline{\left(\theta_{sj} - x/\upsilon\right)} + \upsilon \hat{F}_{xj} \tag{15}$$

where $\overline{\left(\theta_{sj} - x/\upsilon\right)} = \left(\theta_{sj} - x/\upsilon\right)_{ref} - \left(\theta_{sj} - x/\upsilon\right)$.

Controller (15) ensures the convergence of $\left(\dot{x} - \upsilon\dot{\theta}_{sj}\right)$ towards $\left(\dot{x} - \upsilon\dot{\theta}_{sj}\right)_{ref}$.

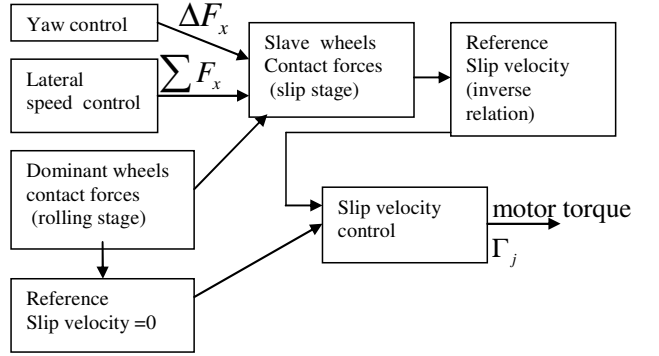The two schemes are summarized in figure 6 and 7.
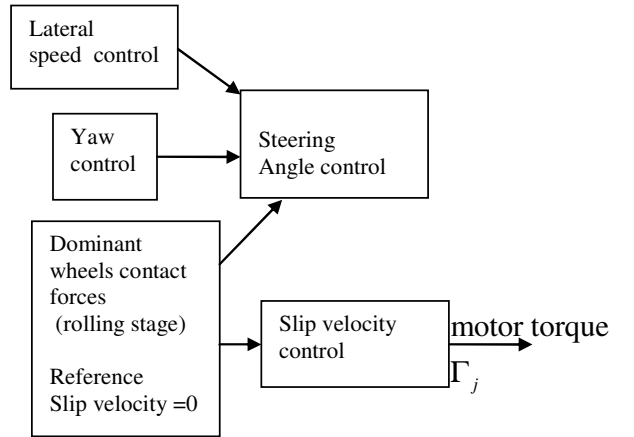

Figure 6. 4X4 control algorithm

Figure 7 Steering actuators plus rolling conditions control algorithm

4. SIMULATIONS

Simulations are carried out with the following parameters: mass $m = 350 \text{ kg}$, wheel radius $\upsilon = 0.2 \text{ m}$, axle track $\rho = 1.4 \text{ m}$, maximum speed $V_{\max} = 5 \text{ m.s}^{-1}$, ellipsoidal inertia $Iz = 46.65 \text{ kg.m}^2$. Simulations are carried out for car misalignement (initial nonzero yaw).

The two control schemes show both their performance and limitations; tuning was achieved by imposing as fast closed-loop poles as possible until equations (8-9)

or (10), depending on the control scheme, could find no solution; a less heuristic procedure has to be found and will be the topic of a future paper. The all 4 X 4 control scheme is actually adequate but performances would deteriorate in case of fault – one sees that the overall speed is reduced in order to recover a proper direction. Control using only steering angles results in a strategy where at first the right angle is tracked at low speed and then a higher speed is reached.
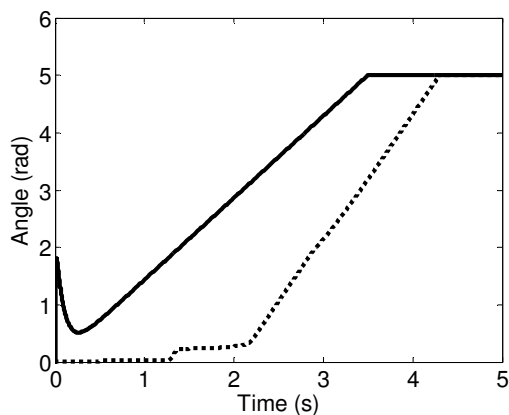

Figure 8 Longitudinal speed
full line: 4x4 monitoring
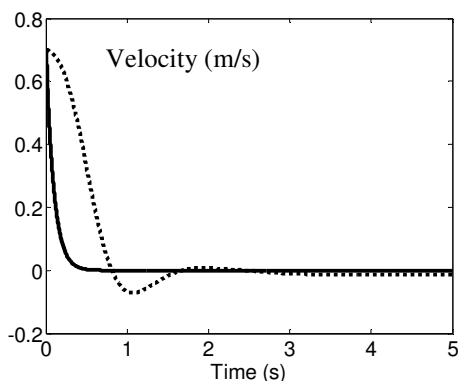dotted line: full steering angle monitoring

Figure 9 Yaw angle
full line: 4x4 monitoring
dotted line: full steering angle monitoring

5. CONCLUSION

Different control algorithms have been proposed for an autonomous overactuated electric vehicle, which owns four actuated traction wheels and two actuated steering systems, based on full 4X4 control or with steering systems control scheme. Preliminary results are given, which show the feasibility of these control algorithms, and the need for a mixed control strategy. Next work will include a generalization of previous results to specific situations (corner crossing, emergency situations, driving on slippery road …) and rapid control reconfiguration (fault in actuators…), allowing to skip from one control scheme to another.

REFERENCES

Merzouki , R., B. Ould-Bouamama , M.A. Djeziri , M. Bouteldja , Modelling and estimation of tire–road longitudinal impact efforts using bond graph approach, *Mechatronics*, 17, 93–108, 2007

Canudas de Wit, C., P. Tsiotras, E. Veenis , M. Basset , G. Gissinger, Dynamic friction models for road/tire longitudinal interaction. *Vehicle Syst Dyn* , 39, 189–226, 2003.

Merzouki, R., M. A. Djeziri, B. Ould-Bouamama, Intelligent Monitoring of Electric Vehicle, 2009 IEEE/ASME International Conference on Advanced Intelligent Mechatronics, Singapore, July 14-17, 2009

Djeziri, M.A., R. Merzouki, B. Ould Bouamama, Robust Monitoring of an Electric Vehicle With Structured and Unstructured Uncertainties, *IEEE Transactions on Vehicular Technology,* 58, 2009

Wang, J., R. G. Longoria, Coordinated and Reconfigurable Vehicle Dynamics Control, *IEEE Transactions on Control Systems Technology*, 17, 2009

Raffo, G.V., G. K. Gomes, J. E. Normey-Rico, C. R. Kelber, L. B. Becker,, A Predictive Controller for Autonomous Vehicle Path Tracking, *IEEE Transactions on Intelligent Transportation Systems*, 10, 2009

Feiqiang, L., W. Jun, L. Zhaodu, Intelligent Speed Adaptation Using a Self-Organizing Neuro-Fuzzy Controller, IEEE Conference on Vehicle Power and Propulsion, Dearborn, MI, 2009.

Partouche D., Pasquier M., Spalanzani A., IEEE Intelligent Vehicles Symposium, Istanbul, 2007

Furukawa, Y., M. Abe, Advanced Chassis Control Systems for the Vehicle Handling and Active Safety. *Vehicle System Dynamics,* 28, 59-86, 1997

Tjønnås, J., T. A. Johansen, Stabilization of Automotive Vehicles Using Active Steering and Adaptive Brake Control Allocation, *IEEE Transactions on Control Systems Technology*, 18, 2010.

Bakker, E., L. Nyborg, H. B. Pacejka A new tyre model with an application in vehicle dynamics studies. *SAE Transactions: Journal of Passenger Cars*, 98(890087), 1989.

Dieulot, J.-Y., F. Colas, Robust PID Control of a linear mechanical axis: a case study, *Mechatronics.* 19 , pp 269-273, 3-2009.

Dumetz E., J.-Y. Dieulot, P.-J. Barre, F. Colas, T. Delplace, Control of an industrial robot using acceleration feedback , *Journal of Intelligent and Robotic Systems*, 46, pp 111–128, 2006.